



U.S. DEPARTMENT OF
ENERGY

Office of
Science

DOE/SC-CM-22-004

FY 2022 Fourth Quarter Performance Metric: Demonstrate Fully Coupled Simulations over the Arctic with Different RRM Configurations and the Impact of High Resolution in the Refined Region

Darin Comeau, Los Alamos National Laboratory (LANL)
Wieslaw Maslowski, Naval Postgraduate School
Stephen Price, LANL
Luke Van Roekel, LANL
Erin Thomas, LANL
Milena Veneziani, LANL
Wilbert Weijer, LANL

October 2022

DISCLAIMER

This report was prepared as an account of work sponsored by the U.S. Government. Neither the United States nor any agency thereof, nor any of their employees, makes any warranty, express or implied, or assumes any legal liability or responsibility for the accuracy, completeness, or usefulness of any information, apparatus, product, or process disclosed, or represents that its use would not infringe privately owned rights. Reference herein to any specific commercial product, process, or service by trade name, trademark, manufacturer, or otherwise, does not necessarily constitute or imply its endorsement, recommendation, or favoring by the U.S. Government or any agency thereof. The views and opinions of authors expressed herein do not necessarily state or reflect those of the U.S. Government or any agency thereof.

Contents

1.0	Product Definition	1
2.0	Product Documentation	1
3.0	Detailed Results.....	5
3.1	Changes in Simulated Ocean Climate	5
3.2	Sea Ice Concentration.....	7
3.3	Transports and Transects.....	8
3.4	Sea Ice Thickness	10
4.0	References	10

Figures

Figure 1.	Ocean and sea ice mesh for <i>InteRFACE</i> and <i>NARRM</i>	2
Figure 2.	Snapshot of surface ocean current speed.....	4
Figure 3.	Annual average of Eddy Kinetic Energy (EKE) for <i>Standard</i> (left), <i>InteRFACE</i> (middle), and observations (right).....	5
Figure 4.	Global sea surface temperature improvements in the Labrador Sea region (white circle) in <i>InteRFACE</i> (middle) relative to <i>Standard</i> (top).....	6
Figure 5.	As in Figure 3 but for the sea surface salinity.	7
Figure 6.	As in Figure 3 but for the mixed layer depth (MLD) in Northern Hemisphere winter.	7
Figure 7.	Northern Hemisphere winter sea ice concentration observations (left), the bias relative to observations (model – observations) from <i>Standard</i> (middle), and the bias relative to <i>InteRFACE</i> (right).....	8
Figure 8.	Velocity (color) and ocean density (contours) through the OSNAP sections (top); observations from Li et al. (2021) (2nd row) and simulation output from <i>Standard</i> (3rd row) and <i>NARRM</i> (bottom row) for the historical period, averaged over 1980-2014.....	9
Figure 9.	Northern Hemisphere winter (February/March) sea ice thickness from <i>Standard</i> configuration (left), <i>HiLAT</i> configuration averaged over years 11-20 (middle), compared against observations (right).....	10

1.0 Product Definition

This report summarizes the improvements in representation of the North Atlantic and arctic climate using coupled versions of the Department of Energy’s (DOE) Energy Exascale Earth System Model (E3SM). E3SM allows for the use of regional refinement in *all* of its components so that high spatial resolution can be focused in specific regions of the globe while maintaining lower resolution in others. This regionally refined mesh (RRM) capability (currently existing in only one other Earth system model; Jungclaus et al. 2022) results in high-resolution model fidelity in regions of interest at a fraction of the computational cost required by a global, high-resolution model. Below, four coupled, E3SM configurations are highlighted: 1) the standard resolution configuration (*Standard*); 2) the Interdisciplinary Research For Arctic Coastal Environments (*InteRFACE*) configuration; 3) the North American RRM (*NARRM*) configuration; 4) the High-Latitude Applications and Testing (*HiLAT*) configuration. The latter three all include RRMs in one or more components to improve deficiencies present in the *Standard* configuration. Each of these is described in more detail in Section 2.

In Section 3, we describe the ability of E3SM’s *Standard* and RRM configurations to resolve important aspects of North Atlantic and arctic climate, including surface ocean currents, eddy-kinetic energy (EKE), sea surface temperature and salinity (SST and SSS, respectively), ocean mixed-layer depth (MLD), sea ice properties, and ocean stratification and velocities along observational transects.

Relative to standard quasi-uniform-resolution E3SM configurations, we show that RRM simulations demonstrate clear improvements in the North Atlantic and the Arctic. These improvements include: (1) the representation of ocean surface currents and EKE, which are critical for accurately resolving heat and salt transport; (2) reduced SST and SSS biases, which are important for accurate representation of ocean vertical mixing and the sea ice cover; (3) reduced biases in MLDs; (4) a reduction in long-standing biases in arctic sea ice concentration, particularly in the Labrador Sea region, and sea ice thickness distribution in the central Arctic; and (5) volumetric transport between the Arctic and North Atlantic ocean basins that is in much better agreement with observations.

2.0 Product Documentation

In this section the E3SM mesh configurations are described. A description of the time domain of each simulation is also given for completeness. The four main configurations that are discussed further in the document are:

1. The standard configuration (hereafter *Standard*) – In the standard configuration, the ocean resolution is 30 km at the Equator and decreases smoothly to 60 km in mid-latitude regions and then increases again to 30 km in high-latitude regions. The design of the base mesh was chosen to fully resolve equatorial wave dynamics and, outside of the tropics, the resolution is such that mesoscale eddies are fully parameterized. The standard atmosphere resolution is uniform at ~100 km.
2. The InteRFACE configuration (hereafter *InteRFACE*) – This configuration uses the standard atmosphere resolution, but couples it to a RRM for ocean and sea ice in which coastal North America, the Arctic, and the North Atlantic are resolved at 14 km. Away from this region, the spatial resolution smoothly transitions back to the ocean and sea ice resolution of *Standard* (Figure 1). This mesh was designed to address science questions (i) under E3SM, pertaining to the changing water cycle in

North America, and (ii) under *InterFACE*, pertaining to how changes in sea ice distributions will impact arctic shipping and economies of the region.

3. The NARRM configuration (hereafter *NARRM*) – This configuration uses the same ocean and sea ice RRM as *InterFACE* and is coupled to an atmospheric RRM that has been refined to 25 km over North America transitioning to the standard 100-km resolution over the rest of the globe.
4. The HiLAT configuration (hereafter *HiLAT*) – This configuration uses an ocean and sea ice RRM with refinement down to 10 km in the Arctic, which smoothly transitions away from this region to the standard resolution. This is paired with an atmosphere RRM with arctic regional refinement down to 25 km, that also transitions to the standard resolution outside this region. Of the four configurations discussed herein, the *HiLAT* and *NARRM* configurations are noteworthy in that they include refinement in the ocean, sea ice, and atmosphere components, currently a new and rare capability among ESMs.



Figure 1. Ocean and sea ice mesh for *InterFACE* and *NARRM*. The light blue area has a grid spacing that varies from 30 km in the equatorial region and Southern Ocean. Throughout the dark blue regions the resolution is 14 km. The coastlines were also modified to ensure critical shipping lanes like the Northwest Passage and Northern Sea Route (shown here in cyan) are open and adequately resolved.

The RRM meshes were designed to answer science questions of the E3SM, *InterFACE*, and *HiLAT* projects. The long-term goal of the Water Cycle campaign is to understand and project changes in water availability over the United States. The *InterFACE* project focuses on how changes in sea ice distributions will impact arctic economies and coastal communities through changes in shipping and resource extraction. The *HiLAT* project focuses on changes in the arctic Earth system, in particular on processes and feedbacks contributing to the accelerated warming of the Arctic known as arctic

amplification. The RRM capability has allowed us to design specific meshes to ensure that critical gateways for arctic-subarctic volume, freshwater, and heat exchanges are realistically represented and that potentially critical shipping routes across the Arctic (i.e., the Northwest Passage and the Northern Sea Routes) are explicitly resolved, at a fraction of the cost of global high resolution. As such, the RRM capability provides a key advantage compared to models at standard resolution, which commonly are limited in representing these arctic gateways and passages, leading to biases in modeled oceanographic and sea ice conditions.

To adequately address critical science questions, the RRM discussed above must not only robustly represent critical processes within the Arctic, but also the lower-latitude processes that affect the Arctic. As an example, heat transport into the Arctic, especially from the Atlantic, exerts a strong control on sea ice thickness and extent. Thus, the Gulf Stream and North Atlantic current must be well represented to accurately capture this oceanic heat transport. An understanding of these key physical processes guided our design of the three refined meshes discussed above, which extend the regions of high spatial resolution to critical regions at lower latitudes.

The *InteRFACE*, *NARRM*, and *HiLAT* RRM were designed to have near-eddy-resolving resolution and eddy-permitting resolution in the Tropics, North Atlantic, and the Arctic. This allows for an improved representation of the Gulf Stream and North Atlantic currents (e.g., Chassignet and Marshall 2008). The improved currents are clearly seen in a snapshot of the surface kinetic energy (Figure 2), where the left panel is for *Standard* and the right panel is from *InteRFACE*. For *Standard*, there are only one or two grid cells across the entire width of the Gulf Stream, resulting in an overly weak current that does not separate from the coast at all, inconsistent with observations. By contrast, for *InteRFACE*, eddy structures in the Gulf Stream region and the subpolar North Atlantic are clearly visible. In particular we note that the separation of the Gulf Stream at Cape Hatteras is consistent with observations and greatly improved over low resolution. Also, the Irminger and Labrador currents are much stronger in *InteRFACE*, which (in addition to contributing to the improvements discussed below) are important for the coupling between the Greenland ice sheet and the Atlantic and Arctic Oceans. The *InteRFACE* mesh increases the number of cells by less than a factor of two while greatly improving the simulation of these currents.

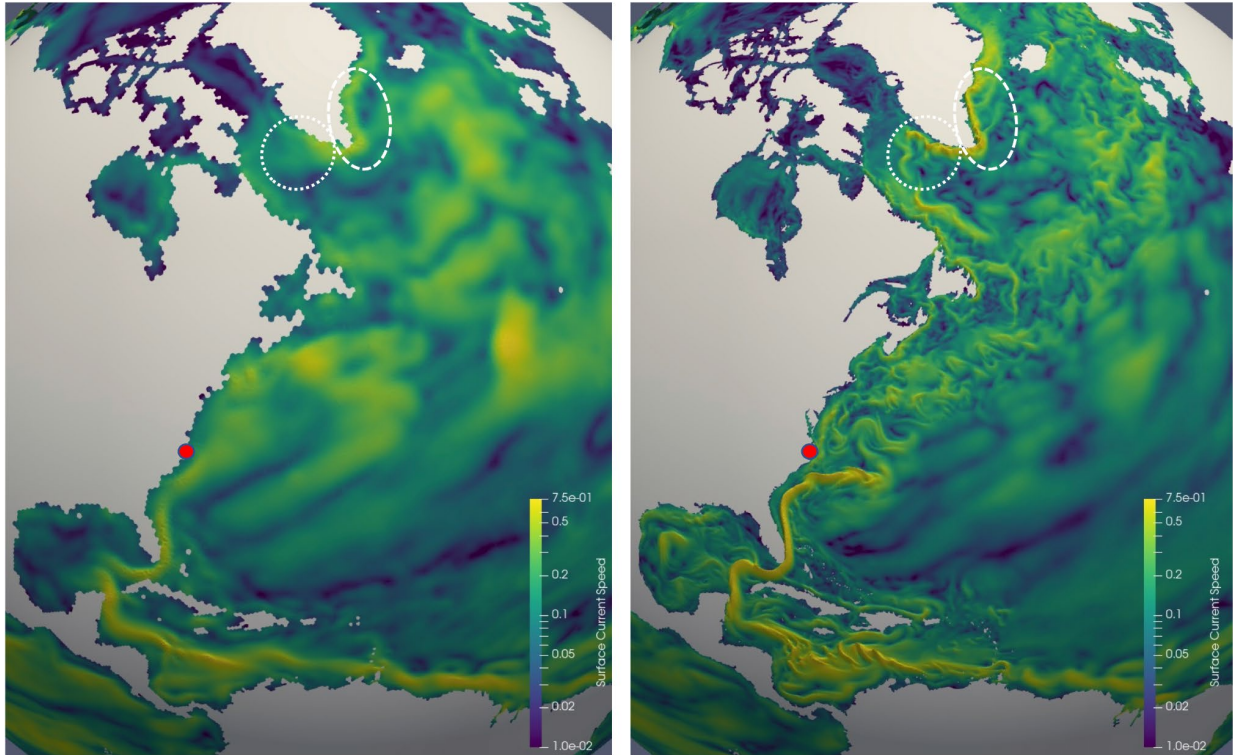


Figure 2. Snapshot of surface ocean current speed. The left panel shows results from *Standard* and the right panel shows results from *InterFACE*. The red circle marks the location of Cape Hatteras. White-dashed and white-dotted circles (respectively) mark the approximate locations of the Irminger and Labrador current improvements.

For all configurations, mesoscale eddies are not fully resolved everywhere, and are represented through the Gent-McWilliams (GM) parameterization (Gent and McWilliams 1990). This parameterization is active in lower-resolution regions where the Rossby radius is not resolved, and inactive otherwise. For *Standard*, GM is fully active for the entire globe. For the arctic-refined configurations, GM is off for resolutions finer than 20 km. This is in the Arctic and subpolar North Atlantic for all configurations, and additionally in the coastal ocean surrounding North America for the *InterFACE* and *NARRM* configurations. The strength of the GM parameterization is linearly tapered to zero as a function of resolution, allowing for the improved representation of heat and mass transport in regions where the increased mesh resolution allows eddies to be resolved.

The *NARRM* and *Standard* configurations have completed 500-year pre-industrial climate control simulations and a 165-year historical period (1850-2015) simulation. The *InterFACE* configuration has completed a 200-year pre-industrial control simulation. The *HiLAT* simulations have so far completed only multi-decadal integrations under fixed 1950 conditions. All simulations were run fully coupled (active atmosphere, ocean, land, and sea ice). Given the unequal simulation lengths, we focus on the shared time period (200 years) for any comparisons involving the *NARRM*, *Standard*, and *InterFACE* configurations. For time series, the full 200 years are analyzed and climatologies are computed over the final 50 years. To compare to observational transects, we also present a climatology over the 1980-2014 period of the E3SM *Standard* and *NARRM* historical period simulations.

3.0 Detailed Results

3.1 Changes in Simulated Ocean Climate

The climatological eddy kinetic energy (EKE) is shown in Figure 3, with *Standard* output in the left panel, *InterFACE* output in the middle panel, and observations in the right panel. Focusing on the North Atlantic, we see a strong increase in EKE in the Gulf Stream and North Atlantic Current and along the southern coast of Greenland (boxed region in figure). The improved EKE is still weaker than observed and this is likely due to a few factors: (1) overly weak wind stress due to coarser atmospheric resolution over the majority of the Atlantic basin, and (2) the North Atlantic resolution is eddy permitting rather than eddy resolving (which would be required to better match observations). Further increases in resolution would likely increase EKE, which would also allow the model to capture features like the Northwest corner, visible in the observations at the entrance to the Labrador Sea. This feature was captured in E3SMv1 where resolution in the region was higher than in any of the model configurations discussed here (Caldwell et al. 2019).

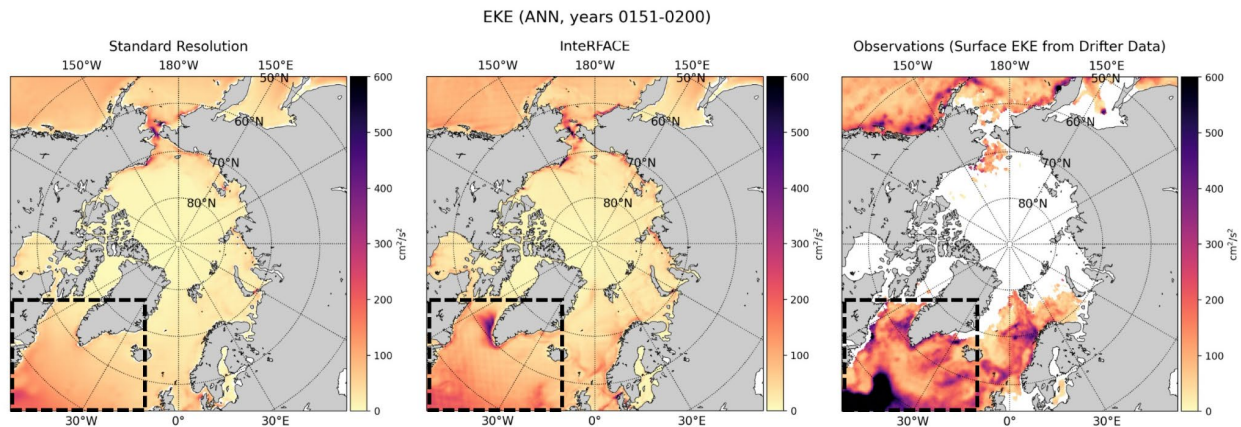


Figure 3. Annual average of Eddy Kinetic Energy (EKE) for *Standard* (left), *InterFACE* (middle), and observations (right).

The increase in fidelity of critical ocean currents is expected to improve the hydrography of the North Atlantic, which would translate to improved SST and SSS. Global SST for Northern Hemisphere winter is shown in Figure 4. Near the Labrador Sea (white-circled region in figure) the SST is significantly warmer in the *InterFACE* simulation relative to the *Standard* simulation. This is due to an improved representation of the subpolar gyre and coastal Greenland currents, which are effective transport mechanisms of very cold and fresh sea ice meltwater away from the Labrador Sea.

SST (JFM, years 0151-0200)

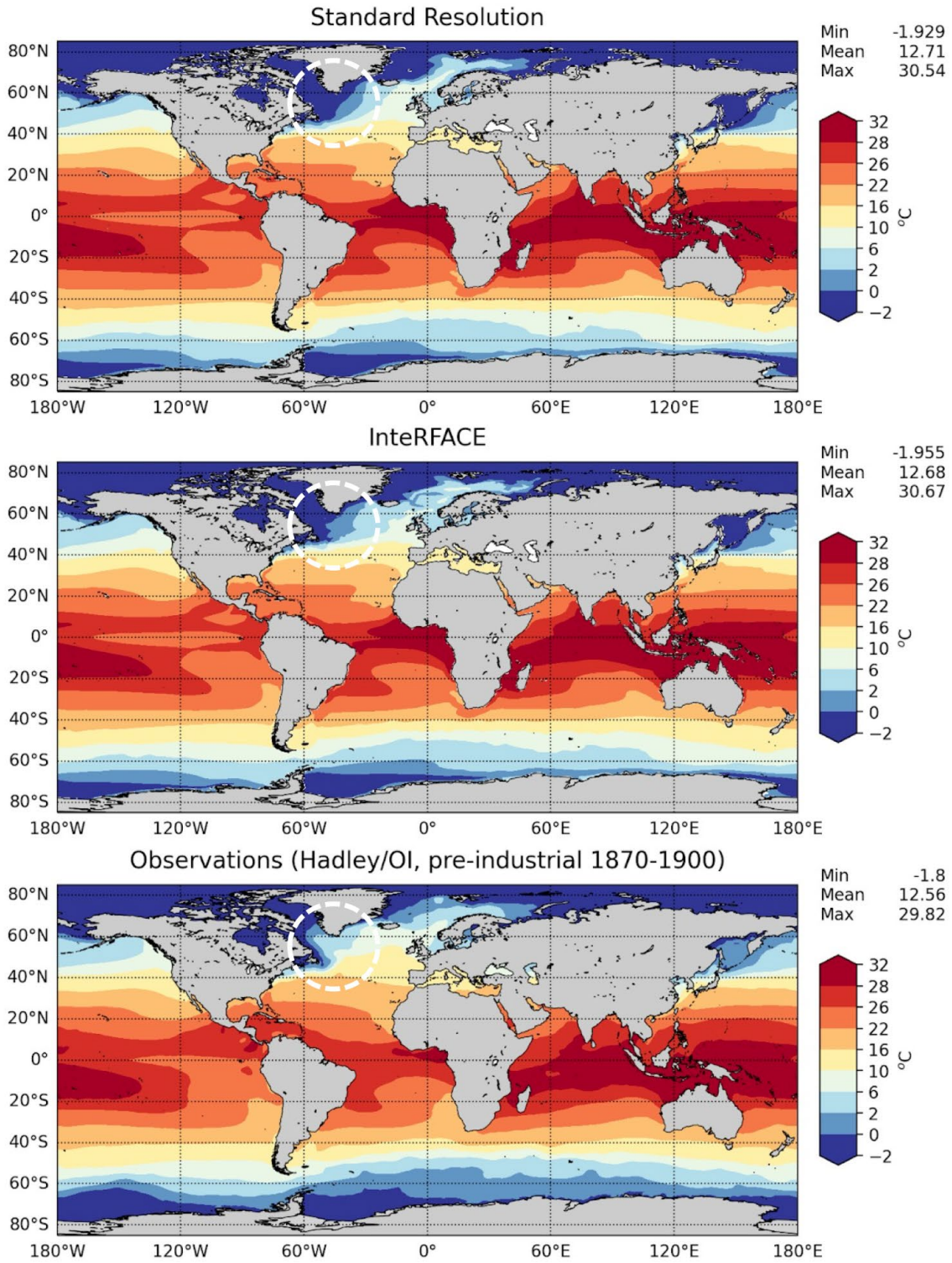


Figure 4. Global sea surface temperature improvements in the Labrador Sea region (white circle) in *InterFACE* (middle) relative to *Standard* (top). Observations for Northern Hemisphere winter (JFM) are shown at bottom.

Figure 5 shows the annual mean sea surface salinity (SSS) simulated in *Standard* (left panel) and *InterFACE* (middle panel). Consistent with the stronger transport previously described, the SSS near the Labrador Sea is significantly improved in *InterFACE* (middle panel) and *NARRM* (not shown). Again, this is due to a more effective transport of surface freshwater input from melting sea ice out of the subpolar region.

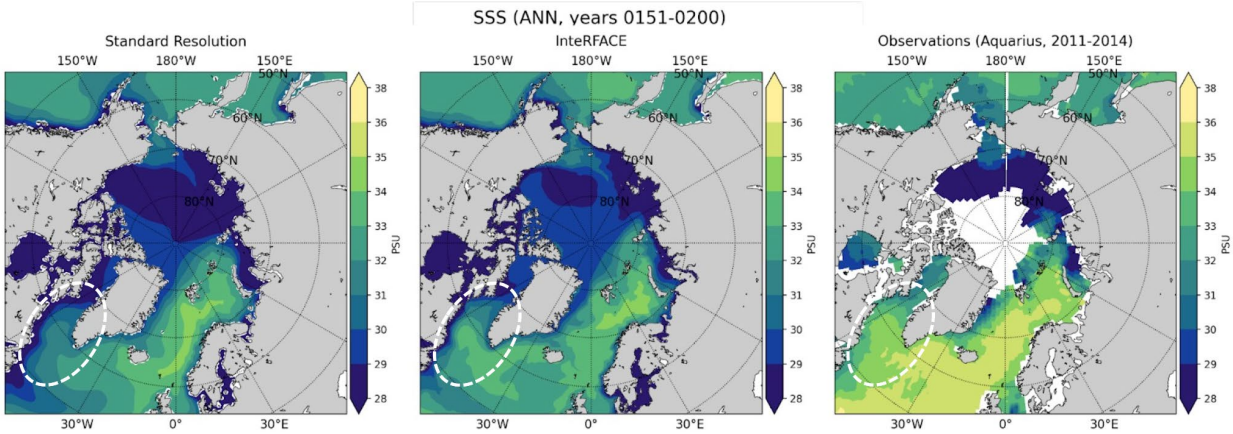


Figure 5. As in Figure 3 but for the sea surface salinity. White ellipse encompasses regions of improved sea surface salinity in the Labrador Sea.

The improvements in SSS and SST in the Irminger sea and subpolar gyre improves the surface density distribution, which in turn improves the simulated MLD in the same region. Figure 6 shows the MLD in winter (January, February, March: JFM) from the *Standard* versus *InterFACE* simulations. Focusing on the western portion of the subpolar gyre (Irminger Sea: white-circled region), we see an increase in the simulated mixed-layer depths.

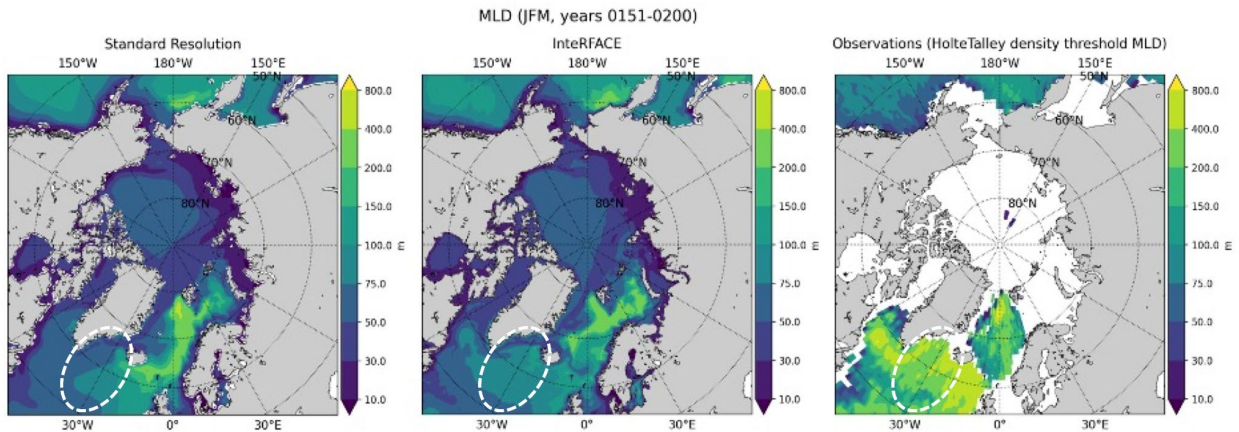


Figure 6. As in Figure 3 but for the mixed layer depth (MLD) in Northern Hemisphere winter. White ellipse encompasses the area of improved MLD in the Irminger Sea.

3.2 Sea Ice Concentration

The near-surface stratification of the ocean – as described by the upper ocean density profile – is strongly correlated with sea ice thickness and extent (e.g., Polyakov et al. 2020). When near-surface waters are extremely fresh, the sea ice is effectively insulated from warmer waters below that inhibit

growth. This leads to a positive feedback and excessive sea ice growth. At low resolution, the weak subpolar gyre and poorly resolved coastal currents around Greenland and Newfoundland are ineffective at removing sea ice meltwater from the Labrador Sea. This in turn makes the Labrador Sea very cold and fresh, leading to excessive sea ice formation through the mechanisms noted above. This cold and fresh bias is clearly seen in Figures 4 and 5. Figure 7 shows the simulated sea ice concentration for Northern Hemisphere winter, with observations in the left panel, the bias relative to *Standard* in the middle, and the bias relative to *InterFACE* on the right. While this figure clearly shows excessive sea ice concentration in the model throughout the Labrador Sea and along the east coast of Greenland (a long-standing issue in many Earth system models including E3SM, see Golaz et al. 2019), the *InterFACE* simulation shows a much-improved sea ice concentration (i.e., a smaller bias) in the Labrador Sea and, to a lesser extent, along the Greenland coast (black-circled regions in figure). The latter is likely due in part to the fact that, as the latitude increases, the *InterFACE* and *NARRM* configurations become less eddy permitting, which reduces heat transport to the region, increasing ice growth. By this understanding, additional increases in resolution in this region can be expected to further reduce the model bias relative to observations.

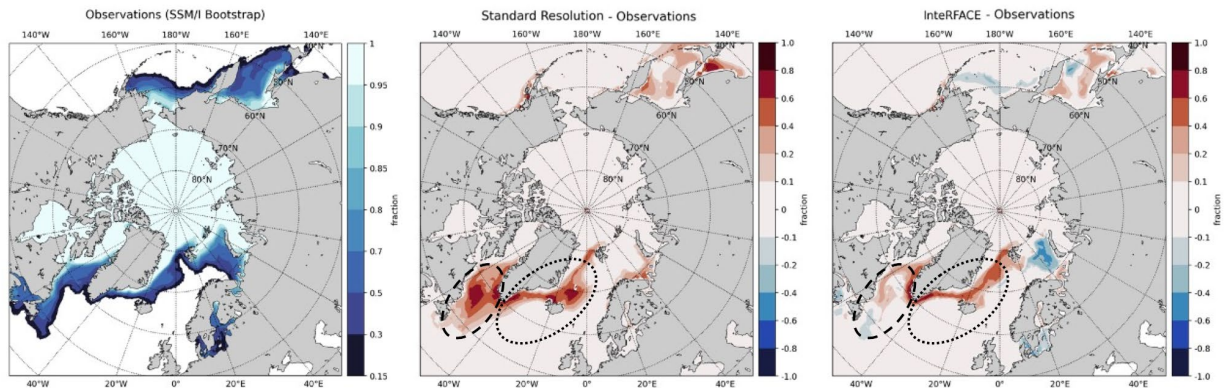


Figure 7. Northern Hemisphere winter sea ice concentration observations (left), the bias relative to observations (model – observations) from *Standard* (middle), and the bias relative to *InterFACE* (right). Black-circled regions focus on improvements in the Labrador Sea (dashed) and along the Greenland coast (dotted).

3.3 Transports and Transects

As mentioned above, the RRM used in the *InterFACE* and *NARRM* configurations was designed to improve the simulation of ice and ocean flow through critical shipping routes that are often closed or unrealistically restricted at low resolution. In Figure 8 we show velocity (as a proxy for volumetric transport) across the Overturning in the Subpolar North Atlantic Program (OSNAP; Li et al. 2021) East and West transects (top panel). In OSNAP West (gray arrows), *NARRM* shows improved coastal currents that are much closer to observations. For OSNAP East (white arrows), the East Greenland current strengthens, and currents associated with bathymetry (e.g., between the Irminger and Icelandic Basins) are much closer to observations, while for *Standard*, these currents are mostly absent.

The density along OSNAP East and West is also improved in *NARRM*. Near the surface, *NARRM* is denser than *Standard*. The volume of higher-density water in the deep ocean has increased in *NARRM*, consistent with an improved representation of bathymetry (Winton et al. 1998). This is seen by comparing the depth of the 27.7 isopycnal contour (bold green line) between *NARRM* and *Standard*; in *NARRM* the depth of this contour has moved toward the surface by a few hundred feet.

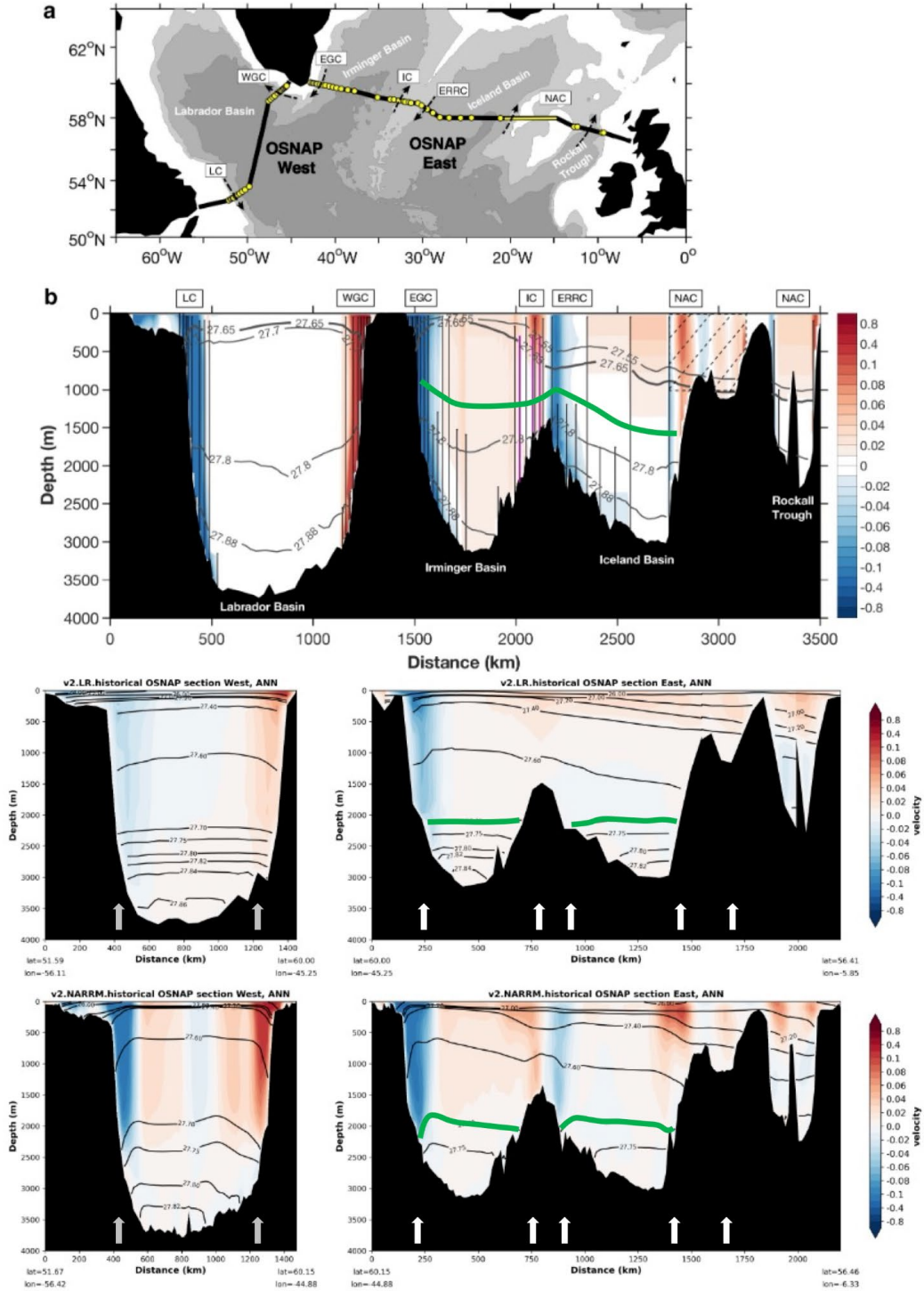


Figure 8. Velocity (color) and ocean density (contours) through the OSNAP sections (top); observations from Li et al. (2021) (2nd row) and simulation output from *Standard* (3rd row) and *NARRM* (bottom row) for the historical period, averaged over 1980–2014. Velocity is perpendicular to the section, with positive (red colors) indicating flow to the northwest for OSNAP West and northward for OSNAP East. The 27.7 isopycnal contour is shown as a bold green line in all cross-sections. Arrows indicate areas where ocean currents are improved in *NARRM* relative to *Standard* along OSNAP West (gray arrows) and East (white arrows).

3.4 Sea Ice Thickness

The *HiLAT* configuration is an arctic-refined configuration of E3SM developed to address the science objectives of the HiLAT-RASM project. Detailed results from a *HiLAT* ocean-and-sea-ice-only configuration were presented in this year's [Q2 metric report](#), which demonstrated improved flux exchange between the arctic and sub-arctic basins (Veneziani et al. 2022). Recently, a fully coupled *HiLAT* configuration has been developed, paired to an arctic atmosphere RRM for improved representation of important patterns of arctic atmospheric circulation, such as arctic cyclones and atmospheric rivers. Simulations with this new configuration are underway and initial results are promising. Figure 9 shows that sea ice thickness distributions in the central Arctic after 20 years of simulation (middle panel) compare much better with the limited satellite estimates of sea ice thickness (right panel). In particular, *HiLAT* demonstrates the buildup of sea ice to the north of the Canadian Archipelago and along the Greenland side of the Arctic (circled region in Figure 9). The lack of thick ice in this region has been a persistent bias seen in the *Standard* configuration (left panel; see also Golaz et al. 2019). Overall, biases in the arctic sea ice thickness distribution are believed to be a major source of a large CMIP6 model spread in representing the past rates of arctic sea ice decline and predictions of its future trends (e.g., Watts et al. 2021).

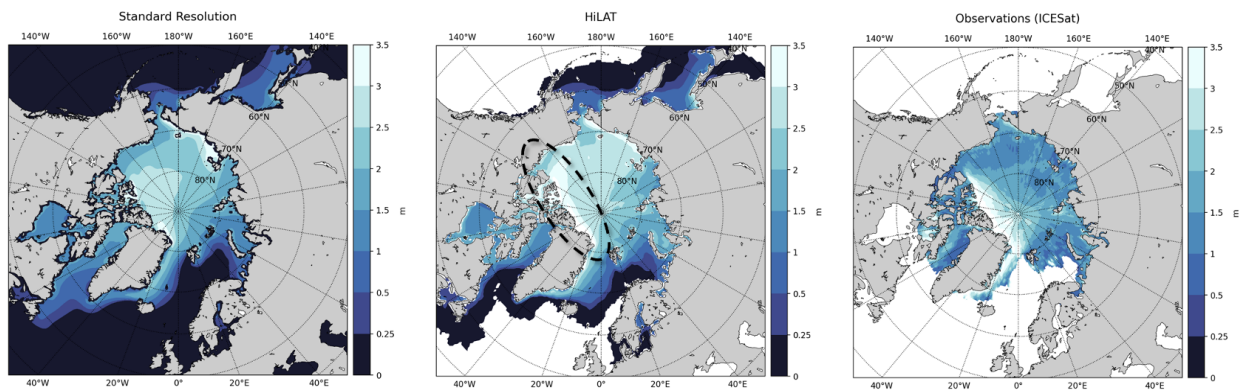


Figure 9. Northern Hemisphere winter (February/March) sea ice thickness from *Standard* configuration (left), *HiLAT* configuration averaged over years 11-20 (middle), compared against observations (right). Note the improved representation of ice thickness on the Canadian Archipelago in the *HiLAT* configuration (circled region).

4.0 References

Caldwell, PM, A Mametjanov, Q Tang, LP Van Roekel, J-C Golaz, W Lin, DC Bader, ND Keen, Y Feng, R Jacob, ME Maltrud, AF Roberts, MA Taylor, M Veneziani, H Wang, JD Wolfe, K Balaguru, P Cameron-Smith, L Dong, SA Klein, LR Leung, H-Y Li, Q Li, X Liu, RB Neale, M Pinheiro, Y Qian, PA Ullrich, S Xie, Y Yang, Y Zhang, K Zhang, and T Zhou. 2019. "The DOE E3SM coupled model version 1: Description and results at high resolution." *Journal of Advances in Modeling Earth Systems* 11(12): 4095–4146, <https://doi.org/10.1029/2019MS001870>

Chassignet, EP, and DP Marshall. 2008. "Gulf Stream separation in numerical ocean models." *Ocean Modeling in an Eddy Regime, Geophysical Monograph Series 177*, <https://doi.org/10.1029/177GM05>

Gent, PR, and JC Mewilliams. 1990. "Isopycnal mixing in ocean circulation models." *Journal of Physical Oceanography* 20(1): 150–155, [https://doi.org/10.1175/1520-0485\(1990\)020<0150:IMIOCM>2.0.CO;2](https://doi.org/10.1175/1520-0485(1990)020<0150:IMIOCM>2.0.CO;2)

Gent, PR, SG Yeager, RB Neale, S Levis, and DA Bailey. 2010. "Improvements in a half degree atmosphere/land version of the CCSM." *Climate Dynamics* 34(6): 819–833, <https://doi.org/10.1007/s00382-009-0614-8>

Golaz, J-C, PM Caldwell, LP Van Roekel, MR Petersen, Q Tang, JD Wolfe, G Abeshu, V Anantharaj, XS Asay-Davis, DC Bader, SA Baldwin, G Bisht, PA Bogenschutz, M Branstetter, MA Brunke, SR Brus, SM Burrows, PJ Cameron-Smith, AS Donahue, M Deakin, RC Easter, KJ Evans, Y Feng, M Flanner, JG Foucar, JG Fyke, BM Griffin, C Hannay, BE Harrop, MJ Hoffman, EC Hunke, RL Jacob, DW Jacobsen, N Jeffery, PW Jones, ND Keen, SA Klein, VE Larson, LR Leung, H-Y Li, W Lin, WH Lipscomb, P-L Ma, S Mahajan, ME Maltrud, A Mametjanov, JL McClean, RB McCoy, RB Neale, SF Price, Y Qian, PJ Rasch, JEJ Reeves Eyre, WJ Riley, TD Ringler, AF Roberts, EL Roesler, AG Salinger, Z Shaheen, X Shi, B Singh, J Tang, MA Taylor, PE Thornton, AK Turner, M Veneziani, H Wan, H Wang, S Wang, DN Williams, PJ Wolfram PH Worley, S Xie, Y Yang, J-H Yoon, MD Zelinka, CS Zender, X Zeng, C Zhang, K Zhang, Y Zhang, X Zheng, T Zhou, and Q Zhu. 2019. "The DOE E3SM coupled model version 1: Overview and evaluation at standard resolution." *Journal of Advances in Modeling Earth Systems* 11(7): 2089–2129, <https://doi.org/10.1029/2018MS001603>

Jungclaus, JH, SJ Lorenz, H Schmidt, V Brovkin, N Bruggemann, F Chegini, T Cruger, P De-Vrese, V Gayler, MA Giorgetta, O Gutjahr, H Haak, S Hagemann, M Hanke, T Ilyina, P Korn, J Kroger, L Linardakis, C Mehlmann, U Mikolajewicz, WA Muller, JEMS Nabel, D Notz, H Pohlmann, DA Putrasahan, T Radatz, L Ramme, R Redler, CH Reick, T Riddick, T Sam, R Schneck, R Schnur, M Schupfner, J-S von Storch, F Wachsmann, K-H Wieners, F Ziemer, B Stevens, J Marotzke, and M Claussen. 2022. "The ICON Earth System Model Version 1.0." *Journal of Advances in Modeling Earth Systems* 14(4): e2021MS002813, <https://doi.org/10.1029/2021MS002813>

Li, F, MS Lozier, S Bacon, AS Bower, SA Cunningham, MF de Jong, B DeYoung, N Fraser, N Fried, G Han, NP Holliday, J Holte, L Houpert, ME Inall, WE Johns, S Jones, C Johynson, J Karstensen, IA Le Bras, P Lherminier, X Lin, H Mercier, M Oltmanns, A Pacini, T Petit, RS Pickart, D Rayner, F Straneo, V Thierry, M Visbeck, I Yashayaev, and C Zhou. 2021. "Subpolar North Atlantic western boundary density anomalies and the Meridional Overturning Circulation." *Nature Communications* 12(1): 3002, <https://doi.org/10.1038/s41467-021-23350-2>

Polyakov, IV, TP Rippeth, I Fer, MB Alkire, TM Baumann, EC Carmack, R Ingvaldsen, VV Ivanov, M Janout, S Lind, L Padman, AV Pnyushkov, and R Rember. 2020. "Weakening of cold halocline layer exposes sea ice to oceanic heat in the eastern Arctic Ocean." *Journal of Climate* 33(18): 8107–8123, <https://doi.org/10.1175/JCLI-D-19-0976.1>

Small, RJ, R Tomas, and FO Bryan. 2014. "Storm track response to ocean fronts in a global high-resolution climate model." *Climate Dynamics* 43(3–4): 805–828, <https://doi.org/10.1007/s00382-013-1980-9>

Veneziani, M, W Maslowski, YJ Lee, G D'Angelo, R Osinski, MR Petersen, W Weijer, AP Craig, JD Wolfe, D Comeau, and AK Turner. 2022. "An evaluation of the E3SMv1 Arctic ocean and sea-ice regionally refined model." *Geoscientific Model Development* 15(7): 3133–3160, <https://doi.org/10.5194/gmd-15-3133-2022>

Watts, MN, W Maslowski, Y Lee, J Clement Kinney, and R Osinski. 2021. "An assessment of Arctic sea ice and regional limitations in CMIP6 historical simulations." *Journal of Climate* 34(15): 1–54, <https://doi.org/10.1175/JCLI-D-20-0491.1>

Winton, M, R Hallberg, and A Gnanadesikan. 1998. "Simulation of density-driven frictional downslope flow in z-coordinate ocean models." *Journal of Physical Oceanography* 28(11): 2163–2174, [https://doi.org/10.1175/1520-0485\(1998\)028<2163:SODDFD>2.0.CO;2](https://doi.org/10.1175/1520-0485(1998)028<2163:SODDFD>2.0.CO;2)



U.S. DEPARTMENT OF
ENERGY

Office of Science